Journal of the Physical Society of Japan
Vol. 71, No. 9, September, 2002, pp. 2164–2168

MHD Instabilities Developing to Alfvén Waves Observed during Plasma Production by MPD Arcjet

Yoshimitsu AMAGISHI, Takanori HISHIDA, Tatsuya INO, Motoshi KOBAYASHI and Akira TSUSHIMA[1]

Department of Physics, Faculty of Science, Shizuoka University, 836 Ohya Shizuoka 422-8529
[1]*Department of Physics, Faculty of Engeneering, Yokohama National University, Yokohama 240-8501*

(Received February 15, 2002)

We have observed two kinds of magnetohydrodynamic (MHD) instabilities excited in a current-carrying cylindrical plasma that was produced by a magneto-plasma-dynamic (MPD) arcjet. The "net current" in the plasma excites the instability with the azimuthal mode number $m = 1$, which is deduced to be a kink mode from MHD theory. On the other hand, the $m = 0$ instability is excited by the "total current" flowing to the cathode, and this mode was found to be responsible for the modulation of electron temperature. They are converted respectively to $m = 1$ compressional Alfvén wave and $m = 0$ global Alfvén eigenmode, propagating along the axial magnetic field in the current-free region.

KEYWORDS: MHD instability, Alfvén wave, kink mode, global Alfvén eigenmode, MPD arcjet
DOI: 10.1143/JPSJ.71.2164

1. Introduction

In a current-carrying plasma, the connection of $m = \pm 1$ kink instabilities with the compressional Alfvén wave (MHD surface wave) or global Alfvén eigenmode (GAE) was first clearly evidenced by Appert *et al.*,[1] by treating the model with a parabolic density profile and a peaked axial current density profile (here we assume wave fields vary as $\exp(ik_z z + im\theta - i\omega t)$). The plasma current introduces an asymmetry about $k_z = 0$ (k_z: wave number along the axial direction) into the dispersion relation at low frequency. Even employing a more simplified model of the plasma,[2] we can see the same unstable region in either side of the dispersion relation, where $\omega^2 < 0$, being identifiied with the kink mode connecting to the MHD surface wave. The MHD surface wave, which was theoretically predicted also in a current-free plasma,[2] was experimentally found, by loading rf power to the antenna, both in a current-free plasma[3,4] and in a current-carrying plasma,[5] but to our knowledge such kink instabilities connected to the Alfvén waves have not been confirmed.

In this paper we present and discuss MHD instabilities, observed during the plasma production by the MPD arcjet which was originally developed as a thruster for space missions.[6] The MPD arcjet was mounted at the end of the linear cylindrical chamber (see §2), and the produced plasma was roughly composed of two parts, i.e. a current-carrying plasma near the MPD source (region I) and almost current-free flowing plasma far from the source (region II), where the net current toward the cathode is considered to be too weak to excite the instability. We observed two kinds of MHD instabilities in the region I with no clear dispersion relations, but they propagate along the axial direction z in the region II with keeping the dispersion relations as well as the azimuthal mode numbers $m = 1$ or $m = 0$. A simplified zero-shear MHD model will make it clarified in §3 that the $m = 1$ mode is the kink instability connected to the compressional Alfvén wave or MHD surface wave, but the $m = 0$ mode, which is connected to GAE, is not explained in the same way as the $m = 1$ mode.

2. Experimental Setup

We have applied the MPD arcjet (Fig. 1) as a plasma source to obtain high plasma densities for the experiments of Alfvén waves, using so far mainly the region II ($z > 0.8$ m) indicated in Fig. 2, where the axial current in the plasma is negligibly small, as will be mentioned in the last paragraph of this section. The cathode diameter of the arcjet is 1.0 cm (tip of the cathode: 0.6 cmϕ) and anode inner diameter 4.0 cm. A singly ionized helium plasma is produced under the axial magnetic field of $B_z = 0.3$ T (ion cyclotron frequency $\omega_{ci} = 7.2 \times 10^6$ rad/sec), and typical plasma density at the center in the region I is $\geq 5 \times 10^{21}$ m^{-3} and $\sim 10^{20}$ m^{-3} in the region II. The electron and ion temperatures in the region II are ~ 5 eV and ~ 20 eV, respectively.

The details of the apparatus and data acquisition system was described elsewhere,[7] but local magnetic fields of fluctuations were measured by using small movable r-, θ-, or

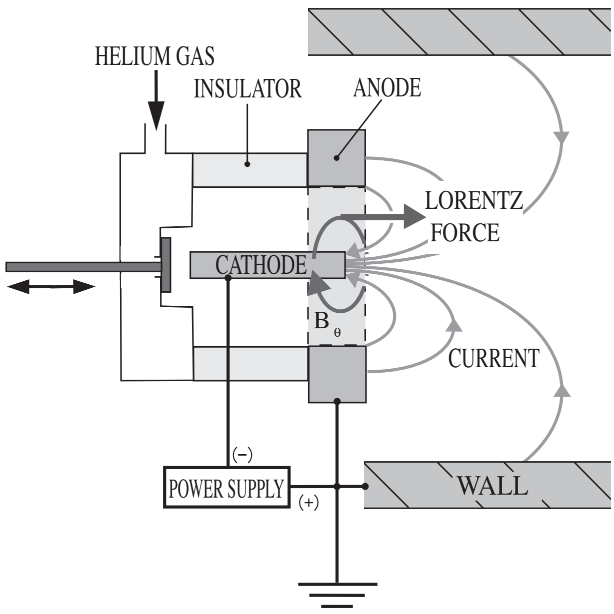

Fig. 1. Schematic drawing of cross section of the MPD arcjet.

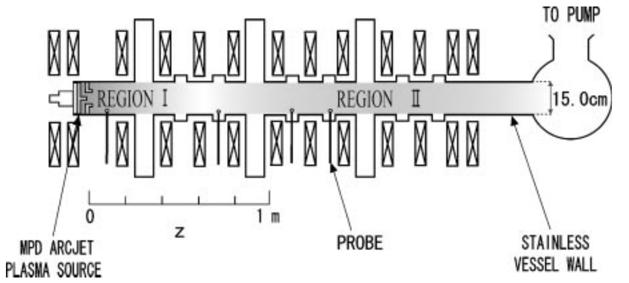

Fig. 2. Schematic of experimental apparatus. It is possible to radially insert movable small magnetic probes, electrostatic single, double and triple probes. The distance z is measured from the MPD arcjet plasma source.

z-magnetic probes consisting of 100 turn-wire with 5 mm in diameter. To estimate the poloidal mode number m, we used two b_z probes azimuthally separated by 90° inserted at the same radius. The data were processed digitally to obtain auto- or cross-power spectrum density, from which dispersion relations and azimuthal mode numbers were calculated. We used single or double probes to measure plasma parameters, i.e. plasma density, electron temperature or floating potetial, and triple probes to measure the fluctuation of electron temperature.

As shown in Fig. 3(a), through the region I the ''total current'' I_T of $-(4.0–4.3) \times 10^3$ A flows about for 1 msec to the cathode from both the anode and conducting wall because the anode is grounded together with the wall. In the plasma cross section near the MPD, the current to the cathode is not canncelled out by that from the anode because of the existence of a current from the wall. This current from the wall or the ''net current'' I_W is $\sim$10% of the total current as shown in Fig. 3(b); the net current density toward the cathode is estimated to be $J_z \sim 5 \times 10^6$ A/m^2. In the region II, however, we observed with magnetic probes the small current density less than 2.5×10^5 A/m^2, flowing toward the cathode only near the plasma center; we could not observed the current density from the anode near $r = 2$ cm. The small current density near the center is then regarded to be from the wall, but too weak to excite any MHD instability.

3. Experimental Results and Discussion

In the region I we have observed two kinds of instabilities, whose frequencies are referred to hereafter as ω_1 and ω_2 ($\omega_1 > \omega_2$). The radial distribution of fluctuating magnetic field $|\delta B_\theta|$ (azimuthal component) at $z = 0.1$ m is exhibited in Fig. 4, and their relation (k_z, ω) is shown in Fig. 5 together with the relation (ω, m). From these figures we find that these are not yet formed as distinct propagating waves, but the group of the frequency ω_1 start to behave like $m = 1$ mode and the group of ω_2 like $m = 0$ mode.

These instabilities are developed in the region II to the propagating waves along the axial magnetic field as seen in Figs. 6 and 7, where the dispersion relations and spectrum of the waves in the region II are shown. It is noted that the waves of ω_1 are $m = 1$ mode, while the waves of ω_2 are $m = 0$ mode, and both groups are located closely on the dispersion relation of the shear Alfvén wave (SAW) at the center in the region II.

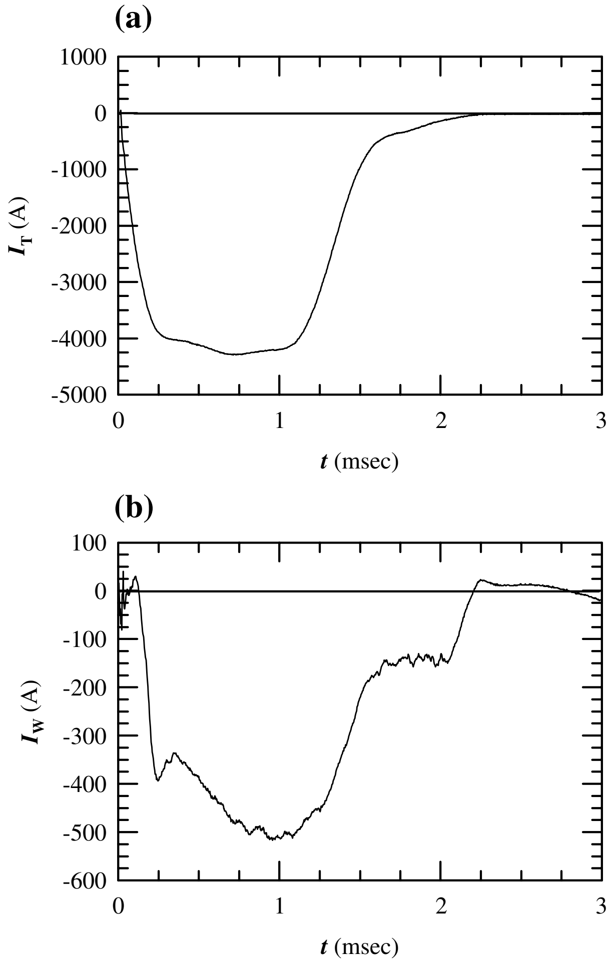

Fig. 3. (a) Total current I_T from the anode and wall, (b) the current I_W from the wall toward the cathode, corresponding to the net current.

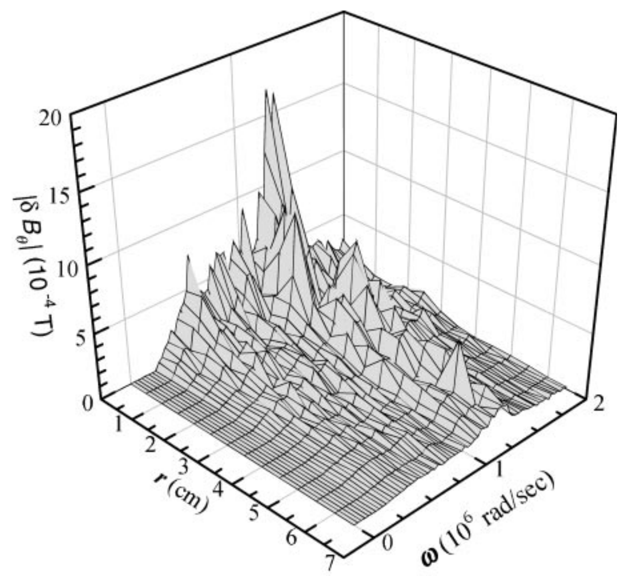

Fig. 4. Radial distribution of fluctuating magnetic field $|\delta B_\theta|$ (azimuthal component) in the region I ($z = 0.1$ m).

3.1 *$m = 1$ mode of group ω_1*

The MHD instability of asymmetric mode $m = 1$, where the azimuthal mode number $m > 0$ for the direction of the electron diamagnetic drift, is nothing but the kink mode, but

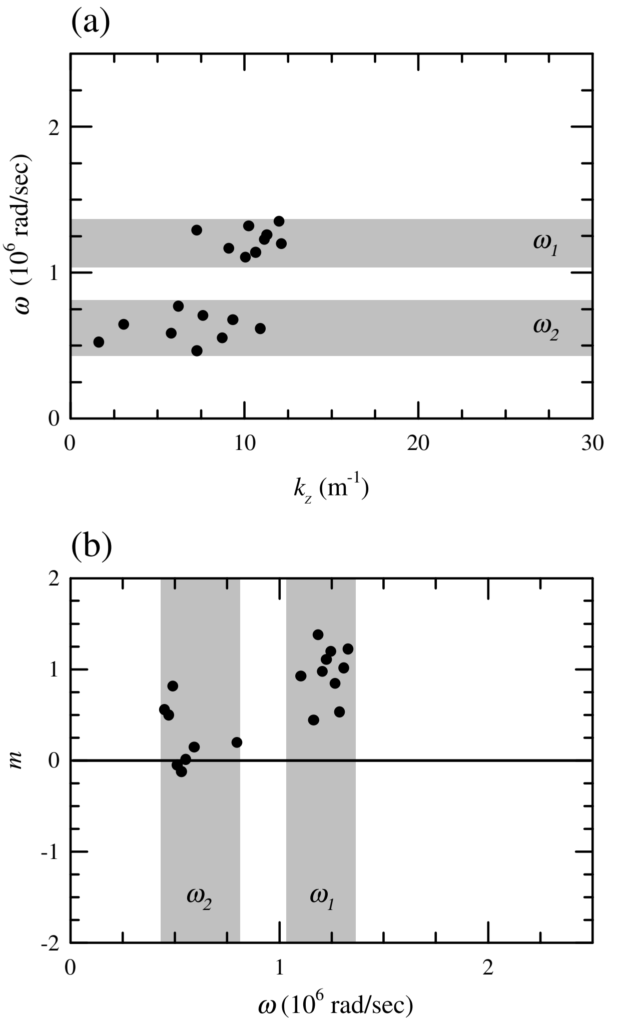

Fig. 5. (a) Dispersion relation and (b) azimuthal mode number m for the oscillations prominent in Fig. 4 ($r = 1.0\,\mathrm{cm}$).

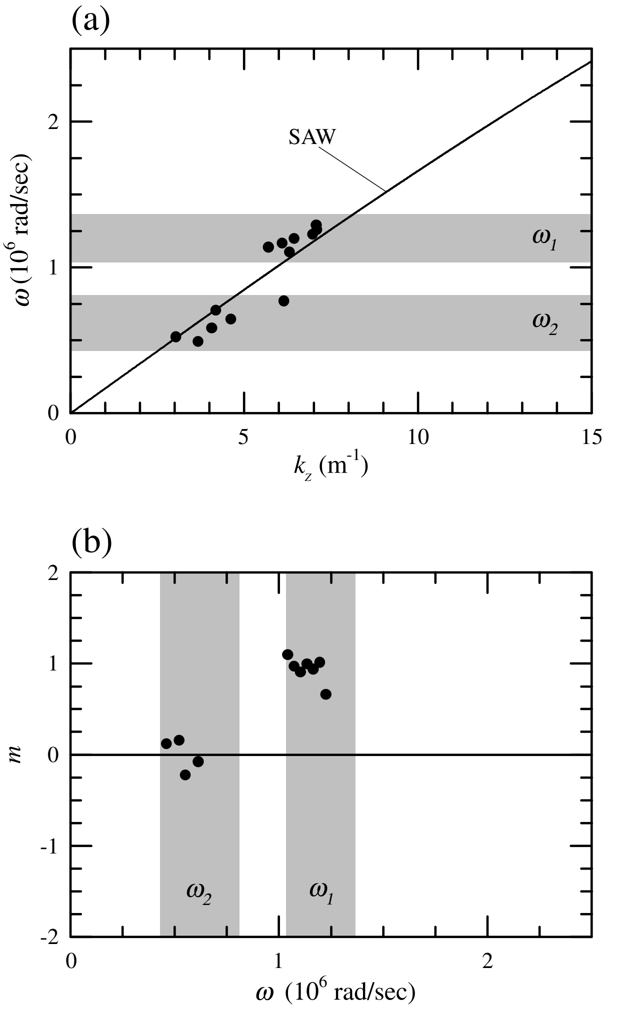

Fig. 7. (a) Dispersion relation of ω_1, ω_2 and (b) azimuthal mode number m, in the region II ($r = 1.0\,\mathrm{cm}$ and $z = 1.3\,\mathrm{m}$). The solid line in (a) represents the dispersion relation of SAW at the center, where the plasma density is $4 \times 10^{20}\,\mathrm{m}^{-3}$.

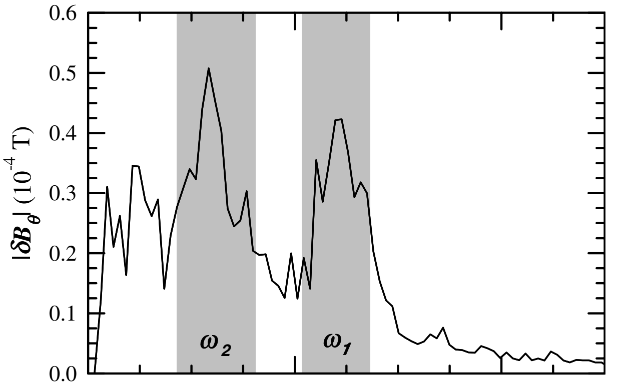

Fig. 6. Spectrum of $|\delta B_\theta|$ for ω_1 and ω_2 in the region II ($r = 1.0\,\mathrm{cm}$ and $z = 1.3\,\mathrm{m}$).

as mentioned above it is converted to the propagating wave in the region II. A great many experiments concerned with Alfvén waves have been performed so far, but nobody has observed $m = 1$ shear Alfvén wave. Hatakeyama *et al.* have reported[8] that the $m = 1$ shear Alfvén wave was observed to be destabilized by a weak field-aligned current, but they defined $m > 0$ for the direction of the ion diamagnetic drift, so that that mode corresponds to $m = -1$ in our definition.

On the other hand, we know that the $m = \pm 1$ compressional Alfvén waves (CAWs) do not suffer from the cutoff frequencies like $m = 0$ mode but exist in the Alfvén continuum region below ω_{ci} if the cylindrical plasma can be modeled with a surrounding vacuum between plasma and wall.[9] Moreover, as shown in Fig. 8, the phase velocity of the observed $m = 1$ mode is almost independent of the inhomogeneous radial plasma density, not as that of the SAW depends on the local density. So we conclude that the observed $m = 1$ mode should be CAW. The $m = 1$ CAW below ω_{ci}, however, does not behave like a surface wave as $m = -1$ mode in the current-free plasma[3] but like a body wave as seen in Fig. 9, and connects to the whistler mode as the frequency increases above ω_{ci}.[2] The group of ω_1 therefore should be located above the dispersion relation of the SAW at the center as the frequency increases.

Next, using the MHD theory, we will substantiate the observed wave number $k_z \sim 7\,\mathrm{m}^{-1}$ for ω_1 in Fig. 7, which must be determined in an unstable region I. According to the Australian group,[2,10] the dispersion relation of MHD waves of low frequency, in a zero shear, current-carrying

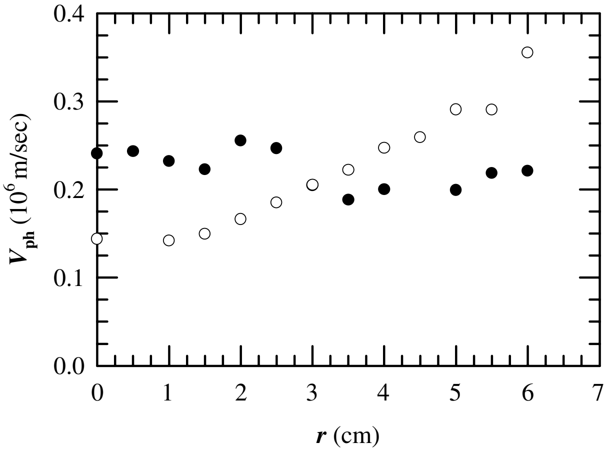

Fig. 8. Phase velocity of the $m = 1$ mode (closed circle), almost independent of the inhomogeneous radial plasma density. For reference the phase velocity of the SAW (open circle), which is excited by a small loop antenna, is shown, depending as expected on the inhomogeneous plasma density in the region II ($z = 1.3$ m).

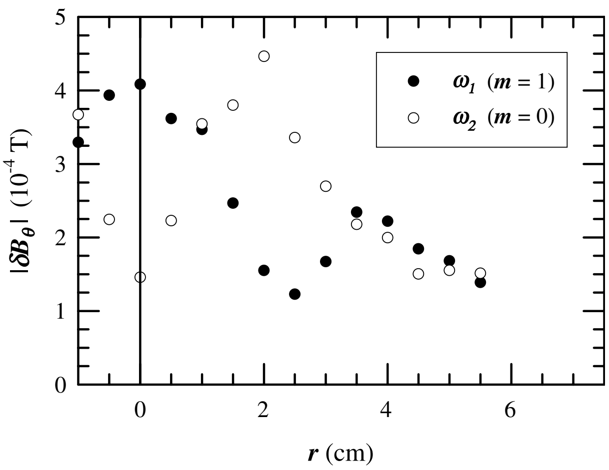

Fig. 9. Radial profile of $|\delta B_\theta|$ of ω_1 and ω_2 in the region II ($z = 1.3$ m).

cylindrical plasma which is surrounded by a vacuum at $r = a$, is derived as follows:

$$\frac{k_\parallel^2}{k_\perp^2}\left[m\left(\frac{G}{F}-1\right)+\frac{k_\perp a J_{m-1}(k_\perp a)}{J_m(k_\perp a)}\right]=\left[\frac{k_z a K_{m-1}(k_z a)}{K_m(k_z a)}+m\right],$$

where $k_\parallel = k_z + m(\mu_0 J/2B_z)$, and F, G are given in refs. 9 and 10. Replacing the vacuum region with another plasma density or wall, we get another different relations.

Let us consider a cylindrical plasma of radius a with constant current density J_z and plasma density n_1, surrounded by another plasma density $n_2 (< n_1)$ with no current up to $r = b$, and a perfect conducting wall at $r = c$. Assuming that a vacuum annulus between b and c exists, and only the net current flows to the cathode through the central plasma of n_1, we obtain the dispersion relation of low frequency $m = 1$ mode as shown in Fig. 10, where the parameters used for calculation are $n_1 = 5 \times 10^{21}\,\mathrm{m^{-3}}$, $n_2 = 5 \times 10^{20}\,\mathrm{m^{-3}}$, $J_z = -5 \times 10^6\,\mathrm{A/m^2}$ and $a = 0.5$, $b = 5.0$, $c = 7.5$ cm.

It is obvious from this figure that an unstable region due to the current, where $\omega^2 < 0$, appears as expected, and the maximum growth rate is given at $k_z \sim 7\,\mathrm{m^{-1}}$, which

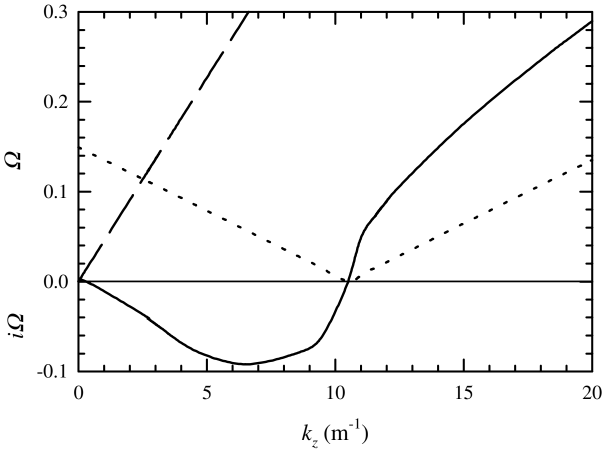

Fig. 10. Dispersion relation of $m = 1$ mode with the unstable kink mode. $\Omega = \omega/\omega_{ci}$. The dotted line shows the dispersion relation of SAW for the density n_1 with the axial current J_z. The dashed line shows that for n_2 with no current.

corresponds to the wave number of ω_1 in Fig. 7(a). Here we used a very simple model with no current effect in the region of the plasma density n_2, but the wavenumber $k_z \sim 7\,\mathrm{m^{-1}}$ agrees with the result obtained by using more realistic model, which will appear elsewhere.

3.2 $m = 0$ mode of group ω_2

The axisymmetric mode $m = 0$ instability is also observed in the region I, and propagates in the region II along the axial direction with the frequency ω_2 as shown in Fig. 7. This mode is located just below or on the dispersion relation of the SAW with the wave number of $k_z \sim 4\,\mathrm{m^{-1}}$, and its azimuthal component of the magnetic field has the peak value around $r = 2$ cm as shown in Fig. 9. The phase velocity of this mode also does not depend on the local plasma density as $m = 1$ described in §3.1, and it is impossible that the MHD surface wave or CAW of $m = 0$ exists below ω_{ci} in the cylindrical plasma surrounded by the wall. In fact we could not excite $m = 0$ mode of the same range of frequency by using antennas, so that observed eigenmode should be a global Alfvén eigenmode (GAE); the $m = 0$ GAE has not been observed yet in screw pinches but it can be usually excited in tokamaks because of poloidal mode coupling effect.[11)]

We can not derive such $m = 0$ instabilities from the same equation with the net current as used for $m = 1$ because much larger current should be required to excite the azimuthal component of magnetic fields and then the assumption $B_\theta \ll B_\parallel$ in that equation is not correct anymore.

If we are allowed, however, to use the same eqaution by assuming that the total current (4.3×10^3 A) toward the cathode is concentrated just in front of the cathode tip of the small radius $r_a = 0.3$ cm and $B_\theta \ll B_\parallel$ is still correct in this area because of $J \times B = 0$, we then obtain an unstable $m = 0$ mode of the wave number $k_z \sim 4\,\mathrm{m^{-1}}$ as shown in Fig. 11, where the dispersion relation of $m = 0$ mode calculated from the simple model is presented. Here we also assumed in the outside of r_a a finite average azimuthal component of the magnetic field due to the central current.

Finally it should be emphasized that the $m = 0$ instability leads to the modulation of electron temperature. In Fig. 12,

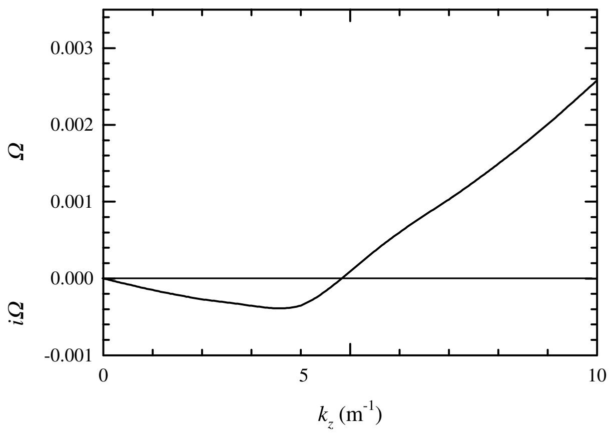

Fig. 11. Dispersion relation of unstable $m = 0$ mode. We assumed that the plasma density ($5.0 \times 10^{21}\,\mathrm{m}^{-3}$) is homogeneous in the radial direction, and the total current concentrated upon the cathode tip, ($J_z = -1.6 \times 10^8\,\mathrm{A/m^2}$), is effective to excite the $m = 0$ mode.

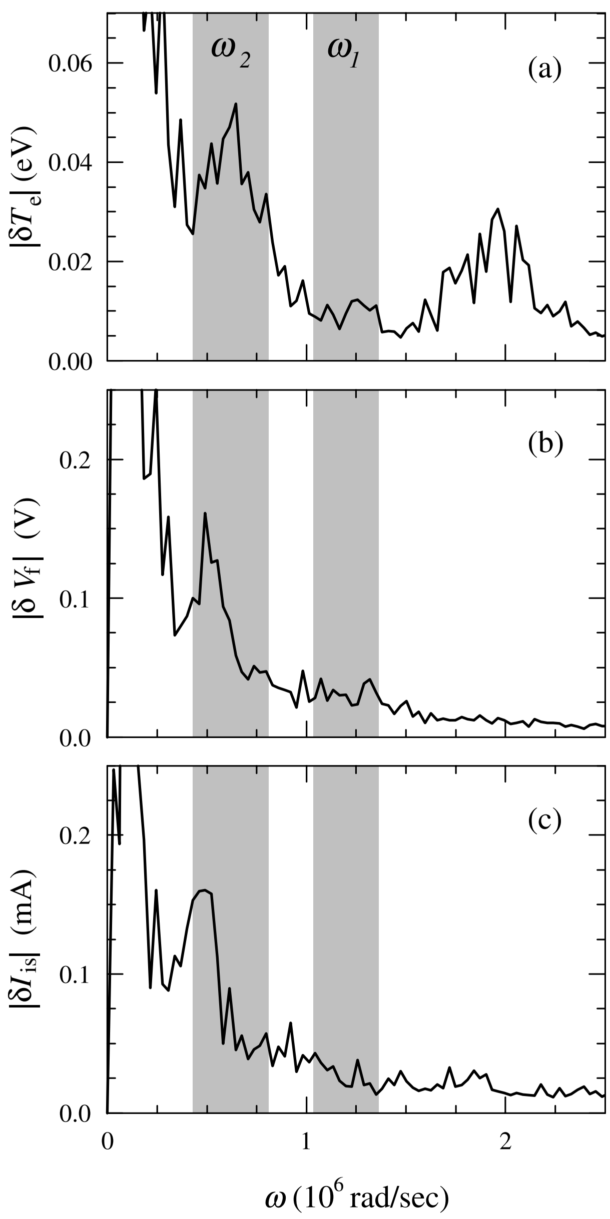

Fig. 12. Modulation of the electron temperature δT_e, floating potential δV_f and ion saturation current δI_{is} as a function of frequency ω ($r = 2.0\,\mathrm{cm}$ and $z = 1.3\,\mathrm{m}$). The modulation mechanism of δT_e at $\omega \sim 2 \times 10^6$ rad/sec is unknown.

absolute fluctuating values of the electron temperature δT_e, floating potential δV_f and ion saturation current δI_{is} are shown as a function of frequency ω. The values of δT_e and others were obtained using a triple probe and a double probe, respectively. Obviously the electron temperature is modulated at the frequency ω_2 but not at ω_1, and this fact reflects to the modulation of the floating potential and ion saturation current, although the peaks are located at slightly different frequencies each other. Taking into account the negligibly small amount of modulation of the total discharge current at ω_2 (less than 1% of the total current, which is almost the same for ω_1), we notice that the $m = 0$ instability or GAE influences the electron temperature, but the investigation concerned with fluctuations of electron temperature by GAW is now under way, so that the detail will be presented in near future.

4. Summary

We have observed the two kinds of MHD instabilities of $m = 0$ and $m = 1$ modes in a current-carrying plasma produced by the MPD arcjet. A simplified MHD theory suggests that it is possible under our experimental conditions for the kink type instability to generate by the net current in a current-carrying plasma, but in the case of the $m = 0$ instability, it is possible only by the total current just in front of thr cathode. We may conclude that these two modes propagate in a almost current-free plasma region as the $m = 1$ CAW and $m = 0$ GAE, respectively. From the experimental fact that the $m = 0$ instability gives rise to the modulation of electron temperature, this mode may be related to the current drive in nuclear fusion devices, or field-aligned current in the magnetosphere.

Acknowledgements

This work is supported in part by Grant-in-Aid for Scientific Research from Ministry of Education, Culture, Sports, Science and Technology.

1) K. Appert, J. Vaclavik and L. Villard: Phys. Fluids **27** (1984) 432.
2) N. F. Cramer and I. J. Donnelly: Plasma Phys. Control. Fusion **26** (1984) 1285.
3) Y. Amagishi: Phys. Rev. Lett. **57** (1986) 2807.
4) Y. Amagishi, K. Saeki and I. J. Donnelly: Plasma Phys. Control. Fusion **31** (1989) 675.
5) G. A. Collins, F. Hofmann, B. Joye, R. Keller, A. Lietti, J. B. Lister and A. Pochelon: Phys. Fluids **29** (1986) 2260.
6) See, for example, A. Sasoh and Y. Arakawa: J. Propulsion Power **8** (1992) 98.
7) Y. Amagishi and A. Tsushima: Plasma Phys. Control. Fusion **26** (1984) 1489.
8) R. Hatakeyama, M. Inutake and T. Akitsu: Phys. Rev. Lett. **47** (1981) 183.
9) G. A. Collins, N. F. Cramer and I. J. Donnelly: Plasma Phys. Control. Fusion **26** (1984) 273.
10) R. Cross: *An Introduction to Alfvén Waves* (Adam Hilger, Bristol and Philadelphia, 1988).
11) A. Elfimov: private comunication, 2001.